

A Synergistic Approach towards Optimization of Coupled Cluster Amplitudes by Exploiting Dynamical Hierarchy

Chayan Patra,^{1, a)} Valay Agarawal,^{2, a)} Dipanjali Halder,¹ Anish Chakraborty,¹ Dibyendu Mondal,^{1, b)} Sonaldeep Halder,^{1, b)} and Rahul Maitra^{1, c)}

¹⁾Department of Chemistry,
Indian Institute of Technology Bombay,
Powai, Mumbai, PIN: 400076, India

²⁾Department of Chemistry,
University of Chicago,
Chicago, IL 60637, USA

The coupled cluster iteration scheme for determining the cluster amplitudes involves a set of nonlinearly coupled difference equations. In the space spanned by the amplitudes, the set of equations are analysed as a multivariate time-discrete map where the concept of time appears in an implicit manner. With the observation that the cluster amplitudes have difference in their relaxation timescales with respect to the distributions of their magnitudes, the coupled cluster iteration dynamics are considered as a synergistic motion of coexisting slow and fast relaxing modes, manifesting a dynamical hierarchical structure. With the identification of the highly damped auxiliary amplitudes, their time variation can be neglected compared to the principal amplitudes which take much longer time to reach the fixed points. We analytically establish the adiabatic approximation where each of these auxiliary amplitudes are expressed as unique parametric functions of the collective principal amplitudes, allowing us to study the optimization with the latter taken as the independent degrees of freedom. Such decoupling of the amplitudes significantly reduces the computational scaling without sacrificing the accuracy in the ground state energy as demonstrated by a number of challenging molecular applications. A road-map to treat higher order post-adiabatic effects is also discussed.

I. INTRODUCTION

Coupled Cluster Theory (CC)¹⁻⁵ is well established electronic structure methodology for accurately solving molecular energetics and properties. In CC method, a correlated wavefunction is generated by the action of an exponential wave-operator involving rank-one (T_1), rank-two (T_2), ..., rank- n (T_n) cluster operators, that act on a suitably chosen reference determinant: $|\psi_{CC}\rangle = e^{T_1+T_2+T_3+\dots}|\phi_0\rangle$. For closed shell cases, the reference determinant ϕ_0 is often taken as the Hartree-Fock determinant and the amplitudes (t) associated with the cluster operators are the unknown quantities that are self-consistently optimized. The cluster amplitudes associated with T_k are determined by projecting a similarity transformed effective hamiltonian $\hat{H}_{eff} = e^{-T}\hat{H}e^T$ against the k -tuply excited determinant that, in principle, folds in the effects of excited determinants such that the correlated ground state energy can be determined as an expectation value of \hat{H}_{eff} with respect to the reference determinant.

CC theory is size-extensive and size-consistent at any level of truncation in the rank of the cluster operators. In this manuscript, without any loss of generality, we would consider the case where only rank-two cluster operators are taken. The resulting CC theory with doubles (CCD) involves coupled optimization of $n_o^2 n_v^2$ amplitudes,

where n_o and n_v are the number of occupied (hole, to be denoted as i, j, k, \dots) and unoccupied (virtual, denoted as a, b, c, \dots) orbitals. Due to the exponential structure of the waveoperator, any optimization strategy involves nonlinearly coupled set of equations among $n_o^2 n_v^2$ amplitudes. This is often done by iterative minimization of a residue vector $R_{ijab} = \langle \phi_{ij}^{ab} | e^{-T} \hat{H} e^T | \phi_0 \rangle$, where $|\phi_{ij}^{ab}\rangle$ is the excited determinant. Thus, at the *fixed point* of the nonlinear optimization process, as $R_{ijab} \rightarrow 0, \forall i, j, a, b, T \rightarrow T_{CCD}$. Note that due to the excitation structure of the cluster operators, the cluster operators are only allowed to contract with the hamiltonian and thus, this optimization procedure scales as $n_o^2 n_v^4$ at the worst.

Due to the nonlinear structure of the working equations, it is alluring to visualize the iterative scheme as a time-discrete multivariate map where “time” enters in an implicit manner with each iterative step being embedded as one discrete-time step. Such iteration scheme undergoes chaotic dynamics when the system of equations is perturbed with an input perturbation. The stability of the equations were, for the first time, demonstrated by Szakács and Surján^{6,7} which is later extended to Lippmann-Schwinger equation⁸. Some of the present authors led the concept one step further to demonstrate that under the influence of single source of perturbation, the nonlinear iteration scheme essentially behaves like a multivariate time-discrete map of one-parameter family⁹ which obeys the universality of the Feigenbaum dynamics^{10,11}. The authors argued the existence of a set of *dominant* collective modes that macroscopically govern the optimization process. Contrarily, there exists large number of other *recessive* variables (amplitudes) that essentially evolve synergistically as dictated by the

^{a)}Contributed equally to the work

^{b)}Authors contributed equally to the work

^{c)}Electronic mail: rmaitra@chem.iitb.ac.in

dominant ones. The present authors, for the first time, exploited the synchronization among the cluster amplitudes during the optimization trajectory via machine learning that resulted tremendous reduction in the degrees of freedom and 40% – 50% savings in computational time to achieve sub-microHartree (μE_h)^{12,13}. As a matter of fact, such a synchronous evolution of all the variables during a (discrete) time evolution is a central theme of Synergetics which gives us a prescription to write the entire dynamics through the collective dominant modes only. Here we briefly explain the concept of nonlinear dynamics and synergetics and how one may apply the concepts of dimensionality reduction for the CC optimization strategy.

In the regions near the fixed point equilibrium, the linear stability analysis enables us to classify the variables into two different sets: the auxiliary (recessive) and principal (dominant) modes^{14,15}. The auxiliary modes are the ones that relax much faster than the principal modes¹⁶, and in the characteristic timescale of the principal modes, one can neglect the time variation of the auxiliary modes (known as Adiabatic Approximation)¹⁷. This is conceptually the generalised version of the Born-Oppenheimer approximation¹⁸. For most of the practical cases the following conditions hold¹⁹:

1. the number of principal modes are much less than than the number of auxiliary modes
2. the magnitude of the principal modes are significantly larger than the magnitude of the auxiliary modes.

Given that the system of variables can be grouped into the auxiliary and principal modes, the “Slaving Principle” enables us to express each of the auxiliary modes as unique function of the principal modes. This thus allows us to confine our attention only to the dynamics of the principal modes. The auxiliary modes unanimously follow the “orders” of the principal modes and therefore, this is known as the master-slave dynamics. With the time evolution of the principal modes, the auxiliary modes also get updated according to their parametric dependence on the principal modes. However, there exists *circular causal* relationship such that the updated information of the auxiliary modes gets coupled back to the dynamical equations of the principal modes, which may be referred to as the feedback coupling¹⁹. The whole dynamical system thus evolves in the interdependent way. As the auxiliary modes at each step merely chip in as a parametric function of the principal modes, the effective degrees of freedom of the whole system is significantly reduced. In one of our previous publications, we developed a first-principle based CC optimization strategy, termed as the Adiabatically Decoupled Coupled Cluster (ADCC), where we have shown that it is possible to distinguish the various amplitudes at their MP2 level into principal and auxiliary modes. Based on certain assumptions which are conceptually close in spirit to the adiabatic approximation, the authors were able to reproduce

very accurate results by optimizing the variables in a reduced subspace²⁰.

The main purpose of this article is to show that some of these features of nonlinear dynamics for the systems close to classical critical points can also be applied in numerically accurate manner (although not mathematically exact) to reduce the computational scaling where nonlinear iterative optimization is involved. We will also demonstrate how the “adiabatic approximation” comes out quite naturally in a more general and rigorous mathematical way, given that some of the cluster amplitudes have significantly longer time scale of relaxation to converge. This will also elucidate the scope to further improve the ADCC results by incorporating some of the higher order post-adiabatic terms^{21,22}. Towards this, we will first present mathematical preliminaries, taking general class of dynamical systems that motivate us towards the development of the adiabatically decoupled CC iterative formulation. We will mainly focus on the underlying concepts of master and slave variables, which are related by the *slaving principle*, and will show how the CC iterative scheme can be adapted within the master-slave dynamics framework for dimensionality reduction. We will show the performance of our model as a function of the dimension of the master modes to justify that CC theory in principle can be optimized in significantly reduced dimension than that dictated by the size of the basis set.

II. ADIABATICALLY DECOUPLED SCHEME FOR COUPLED CLUSTER AMPLITUDE OPTIMIZATION:

A. General Mathematical Preliminaries towards Dimensionality Reduction: Concepts of Adiabatic Approximation and Slaving Principle

As mentioned in the introduction, for specific multivariate dynamical systems, one may divide the entire variable space into auxiliary and principal modes having large difference in their magnitude and characteristic timescale of relaxation. In order to have an easy readability, in the following, we first discuss the mathematical preliminaries that allow us to express the dynamics of the whole system solely in terms of the principal modes. We will consider a general dynamical system with continuous time variation. The corresponding discrete analogue pertinent to the CC iterative scheme will be developed in the next subsection.

Let us consider a multivariate dynamical system $\{\hat{\mathbf{q}}\}$ evolving according to the following general form of an equation:

$$\dot{\hat{\mathbf{q}}} = L\hat{\mathbf{q}} + \mathbf{N}(\{\hat{\mathbf{q}}\}) \quad (1)$$

where, L is a coefficient matrix independent of the dynamical variables and \mathbf{N} contains all the nonlinear couplings among them. One may perform a linear stability

analysis^{23–25} to obtain a set of eigenvalues $\{\lambda\}$ of the stability matrix that can be classified into the following two categories.^{19,22}

$$\begin{aligned} \{\lambda_u\} &\geq 0; & (\text{total number } N_u) \\ \{\lambda_s\} &< 0; & (\text{total number } N_s) \end{aligned} \quad (2)$$

with the condition:

$$|\lambda_{s_i}| > |\lambda_{u_I}| \quad (3)$$

In the usual scenario, $N_s \gg N_u$, where the individual elements from the sets of eigenvectors of λ_u ($\{u\}$) and λ_s ($\{s\}$) are denoted by u_I and s_i . Positive values of λ_u indicates the dynamics is non-equilibrium and the corresponding eigenvectors are the unstable modes which move away from the fixed point as time progresses²⁴. This justifies the subscript u and s referring to unstable and stable modes, respectively. On the other hand, keeping in mind the CC iteration dynamics, we are only interested here in the negative λ_u cases, referring to an overall equilibrium system that eventually reaches one of the fixed points of the dynamics. This indicates that all the λ s can be considered as damping factors. Hence, we drop the terminology of unstable and stable modes from here on, rather we keep the same subscripts but prefer to refer them in a more general way as the *principal* and *auxiliary* modes. In the transient period, the variables with smaller and larger amplitudes generally have larger and smaller damping factors respectively, allowing us to establish a demarcation between auxiliary and principal amplitudes. The nonlinearly coupled equations of motion for these two sets of amplitudes can be written as:

$$\dot{u}_I = \lambda_{u_I} u_I + Q_I(u, s); \quad \text{where } I = 1, 2, \dots, N_u \quad (4)$$

and

$$\dot{s}_i = \lambda_{s_i} s_i + P_i(u, s); \quad \text{where } i = 1, 2, \dots, N_s \quad (5)$$

Here Q_I , P_i contains all the information of nonlinearity and inter-mode coupling. In a narrow region around a fixed point (i.e. $\{\dot{u}_I\}, \{\dot{s}_i\} = 0$) where linearization can be applied, one may analyze the dynamics by neglecting the small contributions from the nonlinear terms in Q_I and P_i . In such a scenario, when the system is perturbed slightly from the fixed point equilibrium, the whole system moves under the influence of the principal modes $\{u_I\}$ in their characteristic timescale, whereas, the auxiliary modes $\{s_i\}$ decay back to the fixed point. In other words, s_i can be considered as heavily damped modes whereas u_I is relatively under-damped.

By exploiting the characteristic relaxation timescale, we wish to show that s_i amplitudes can be expressed by means of u_I only, such that one can also eliminate $\{s_i\}$ from Eq. (4) by direct substitution. The most general solution to Eq. (5) can be obtained as

$$\begin{aligned} \left(\frac{d}{dt} - \lambda_{s_i}\right) s_i &= P(u, s) \\ \implies s_i &= \left(\frac{d}{dt} - \lambda_{s_i}\right)^{-1} P(\{u, s\}) \end{aligned} \quad (6)$$

The inverse differential operator can be solved with an integral form that allows us to write²²:

$$s_i(t) = \int_{-\infty}^t e^{\lambda_{s_i}(t-\tau)} P(\{u, s\}) d\tau \quad (7)$$

Assuming the integral is finite and well-behaved^{26,27}, one may perform an integration by parts to further simplify Eq. (7)

$$s_i(t) = -\frac{1}{\lambda_{s_i}} P(\{u, s\}) - \frac{1}{(-\lambda_{s_i})} \int_{-\infty}^t e^{\lambda_{s_i}(t-\tau)} \left(\frac{d}{d\tau} P\right) d\tau \quad (8)$$

The second term in right hand side onward are usually very small. Hence, neglecting the small higher order terms, Eq. (8) reads

$$s_i(t) = -\frac{1}{\lambda_{s_i}} P(\{u, s\}) \quad (9)$$

A careful observation leads to the interesting fact that we can avoid all the mathematical jargon and still get the same result as that of Eq. (9) if we simply set $\dot{s}_i = 0$ in Eq. (5). This simply implies that in the characteristic time scale of the principal modes, the time-variation of the auxiliary modes can be neglected. This is to be referred as the *adiabatic approximation*.

Generally in all practical cases, the amplitude of the principal modes are extremely large in comparison to auxiliary modes. Thus all the contributions from s_i can be neglected compared to u_I such that the right hand side of Eq. (9) can be written as a function of u_I alone, which simplifies the expression as:

$$s_i(t) = -\frac{1}{\lambda_{s_i}} P(\{u\}) \quad (10)$$

As we have the expression in Eq. (10) for the auxiliary modes as a function of the principal modes, we can now imitate the system dynamics in a reduced subspace spanned only by the principal modes, which are much fewer in number compared to the auxiliary modes. In the context of CC iterative approach, our goal is to accurately determine s as a function of $\{u\}$ only, which would be fed back to the dynamics of $\{u\}$ to get an updated set of principal modes. This loop, referred to as the *circular causality loop*, would continue till the principal modes converge below a pre-defined threshold.

B. Coupled Cluster iterative optimization from the synergistic viewpoint:

We now turn our attention to the optimization of CC theory using Jacobi iterative scheme. We would consider the iterative scheme as a time-discrete map where each iteration is embedded as one time step. Furthermore, since the iterative optimization leads to a set of fixed points, it can be considered as an equilibrium system from the perspective of nonlinear science, and hence the demarcation

of the auxiliary and principal modes (as shown in Eq. (2) for non-equilibrium systems) does not strictly hold according to the linear stability analysis⁹. In general, for equilibrium systems (in the perspective of nonlinear dynamics), all the values of λ may be negative; however, for all practical purposes, one may bypass the linear stability criteria and classify the amplitudes based on their distribution of magnitudes into auxiliary and principal modes having shorter or longer characteristic relaxation time to reach their fixed point solutions. We will generally refer to these amplitudes as auxiliary and principal amplitudes, respectively.

With the approximations in mind, let us now consider the amplitudes updating Jacobi equation

$$\begin{aligned} \Delta t_\mu &= t_\mu^{(k+1)} - t_\mu^k = \frac{R_\mu}{D_\mu} \\ &= \frac{1}{D_\mu} (H_\mu + \overline{(HT)}_\mu) + \frac{1}{2} \overline{(HTT)}_\mu \end{aligned} \quad (11)$$

Here T is the cluster operator, t_μ denotes the associated amplitudes with hole-particle excitation structure ' μ ' and R_μ is the corresponding residue. The hamiltonian H contains the one and two electron terms. It was observed from a number of numerical examples²⁰ that the amplitudes with large magnitude (at the MP2 level) take substantially more number of iterations to reach their converged values (fixed points) than the ones with smaller magnitudes. Based on the relative magnitude of these amplitudes, the entire amplitude space can be subdivided into a Large Amplitude Subset (*LAS*, spanned by $\{T_L\}$ with dimension n_L) and Small Amplitude Subset (*SAS*, spanned by $\{T_S\}$, with dimension n_S). In our time-discrete iterative map, their amplitudes $\{t_L\}$ plays the role of the principal modes and $\{t_S\}$ plays the role of the auxiliary modes. Note also that $n_S \gg n_L$ and $|t_L| \gg |t_S|$. They will thus be referred to as the *principal* and *auxiliary* amplitudes, respectively. In conjunction to the dynamics of the principal and auxiliary modes shown in Eqs. (4) and (5), the same for the principal and auxiliary amplitudes can be written as:

$$\Delta t_{L_I} = \frac{1}{D_{L_I}} \overline{(H_{L_I}^d T_{L_I})}_{L_I} + Q_{L_I}(\{T_L, T_S\}); \forall I = 1, 2, \dots, n_L \quad (12)$$

and

$$\Delta t_{S_i} = \frac{1}{D_{S_i}} \overline{(H_{S_i}^d T_{S_i})}_{S_i} + P_{S_i}(\{T_L, T_S\}); \forall i = 1, 2, \dots, n_S \quad (13)$$

where, L_I and S_i are composite hole-particle indices for *LAS* and *SAS* elements, respectively. D_μ is the corresponding orbital energy difference for the general hole-particle index μ . Here Q_{L_I} and P_{S_i} contain all the information of nonlinearity for the dynamics of the principal

and auxiliary amplitudes, and they can be expanded as:

$$\begin{aligned} Q_{L_I}(\{T_L, T_S\}) &= \frac{1}{D_{L_I}} \left[\overline{(H_{L_I} + \overline{(HT_{L_J})}_{L_I} + \overline{(HT_{S_i})}_{L_I})} + \right. \\ &\left. \frac{1}{2} \overline{((H T_{L_J} T_{L_K})_{L_I} + (H T_{L_J} T_{S_i})_{L_I} + (H T_{S_i} T_{S_j})_{L_I})} \right] \end{aligned} \quad (14)$$

and

$$\begin{aligned} P_{S_i}(\{T_L, T_S\}) &= \frac{1}{D_{S_i}} \left[\overline{(H_{S_i} + \overline{(HT_{L_I})}_{S_i} + \overline{(HT_{S_j})}_{S_i})} + \right. \\ &\left. \frac{1}{2} \overline{((H T_{L_I} T_{L_J})_{S_i} + (H T_{L_I} T_{S_j})_{S_i} + (H T_{S_j} T_{S_k})_{S_i})} \right] \end{aligned} \quad (15)$$

Here the *diagonal* terms, H^d , in Eqs. (12) and (13) needs some explanation. The diagonal part of the hamiltonian matrix H_μ^d are the composite tensorial terms which upon contraction with T_μ generate a structure with hole-particle composite structure as μ . The diagonal part is extracted out in the expressions of Δt_μ in Eqs. (12) and (13) to show their one-to-one correspondence with Eqs. (4) and (5). The explicit expression for H_μ^d is given by

$$\begin{aligned} H_\mu^d &= (1 + P(i, j)P(a, b)) \left(-f_{ij} + f_{aa} + \frac{1}{2}v_{ab}^{ab} + 2v_{ia}^{ai} \right. \\ &\quad \left. - (1 + \delta_{ij}\delta_{ab})v_{ia}^{ia} + \frac{1}{2}v_{ij}^{ij} - v_{ib}^{ib} \right) \\ \mu &= \{ijab\} \in SAS \text{ or } LAS \end{aligned} \quad (16)$$

Here i, j refer to the occupied (hole) orbital indices while a, b refer to the unoccupied (particle) orbital indices. The canonical Fock operator matrix elements and the two electron integrals are represented by f and v respectively, and P is the permutation operator.

We are now in a position to develop the discrete-time analogue of Eq. (7) for the CC optimization. Without going into the details of the equation, for which we refer to Haken^{15,28}, the most general solution for the auxiliary amplitudes, t_S , can be written as:

$$t_{S_i} = \sum_{m=-\infty}^l (1 + \lambda_{S_i})^{l-m} P_{S_i} \quad (17)$$

where,

$$\lambda_{S_i} = \frac{H_{S_i}^d}{D_{S_i}} \quad (18)$$

Note that $H_{S_i}^d$ and D_{S_i} have opposite sign (and hence CC equations form a convergent series) and thus λ_{S_i} is negative. The expression in the right hand side of Eq. (18) can be expanded using *summation by parts*, a mathematical trick similar to integration by parts of Eq. (8),

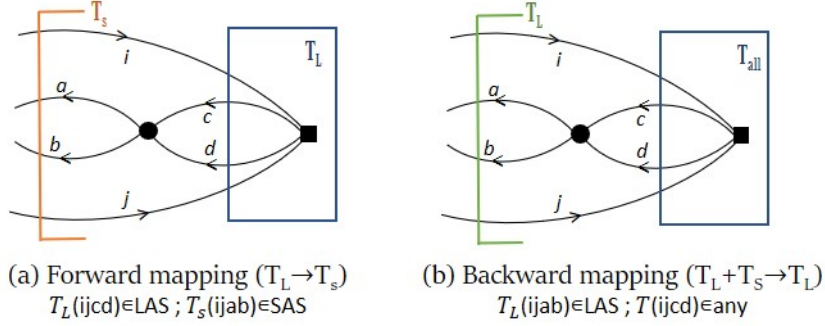


FIG. 1. Representative diagrams contributing to the leading order of computational scaling. Diagrams of the same topology are shown for forward mapping (a) and backward mapping (b) with different interpretation.

to obtain:

$$\begin{aligned}
t_{S_i} &= P_{S_i} \sum_{m=-\infty}^l (1 + \lambda_{S_i})^{l-m} \\
&- \sum_{m=-\infty}^l (1 + \lambda_{S_i})^{l+1-m} \sum_{m'=-\infty}^{m-1} (1 + \lambda_{S_i})^{m-1-m'} \Delta P_{S_i}
\end{aligned} \quad (19)$$

Here, “ Δ ” is the time-discrete version of the time derivative operator “ d/at ”. Since the auxiliary modes have $\lambda_{S_i} < 0, \forall S_i$, one can simplify the intricate summations above using the identity:

$$\sum_{m=-\infty}^l (1+x)^{l-m} = -\frac{1}{x}; \quad |x+1| < 1 \quad (20)$$

The simplification of Eq. (19) leads to

$$t_{S_i} = \underbrace{-\frac{P_{S_i}(\{t_L, t_S\})}{\lambda_{S_i}}}_{\text{adiabatic}} - \underbrace{\frac{\Delta P_{S_i}(\{t_L, t_S\})}{\lambda_{S_i}^2}}_{\text{post-adiabatic}} \quad (21)$$

We will briefly explain the significance of these two terms that appear on the right hand side of Eq. (21). As mentioned previously, one may neglect the time variation of the auxiliary modes (auxiliary amplitudes) in the characteristic timescale of the principal modes (principal amplitudes). By setting up the condition $\Delta t_{S_i} = 0$ to neglect the time variation of the auxiliary amplitudes, one obtains the first term on the right hand side of Eq. (21). This thus can be interpreted as the *adiabatic approximation*. Note that in one of our earlier publications²⁰, the adiabatic approximation was introduced simply by setting the decoupling condition. Here we further corroborate the concept by introducing a discrete-time dependent picture and timescale decoupling in the amplitude space. The second term on the right hand side of Eq. (21) depends on the discrete-time variation of the (part of the) residue P_{S_i} and depends on $\lambda_{S_i}^2$. This thus may be interpreted as post-adiabatic correction and will not be

considered in this article any further. We will introduce the post-adiabatically corrected optimization scheme in our future publication.

In what follows, we will now proceed exactly the same way that allowed us to derive Eq. (10) from Eq. (9). Noting the fact²⁰ the auxiliary amplitudes t_S are significantly small compared to the principal amplitudes, t_L , one may neglect t_S from the adiabatically decoupled expression of t_{S_i} :

$$t_{S_i(ad)} = -\frac{P_{S_i}(\{t_S, t_L\})}{\lambda_{S_i}} \xrightarrow{|t_S| \approx 0} -\frac{P_{S_i}(\{t_L\})}{\lambda_{S_i}} \quad (22)$$

or in the long hand notation by writing $P_{S_i}(\{t_L\})$ explicitly:

$$t_{S_i(ad)} = -\frac{1}{H_{S_i}^d} \left[H_{S_i} + \overline{(HT_{L_I})}_{S_i} + \frac{1}{2} \left(\overline{(HT_{L_I} T_{L_J})}_{S_i} \right) \right] \quad (23)$$

where all the terms that involve T_S are set to zero. We note that setting the adiabatic condition $\Delta t_{S_i} = 0$ does not imply that the auxiliary amplitudes are frozen to given pre-computed values. Rather, they are updated through parametric functional dependence on the principal amplitudes. We now turn our attention to the computation of the determination of the principal amplitudes via feedback coupling.

Feedback coupling and the determination of the principal amplitudes:

As previously mentioned, there exists circular causality relationship among the principal and the auxiliary amplitudes. This implied that the updated information of the auxiliary amplitudes (obtained from Eq. (23)) must get fed back to the updating equations for T_L . Noting the fact that $T_{S_i(ad)} = T_{S_i}(\{t_L\})$, one may explicitly write

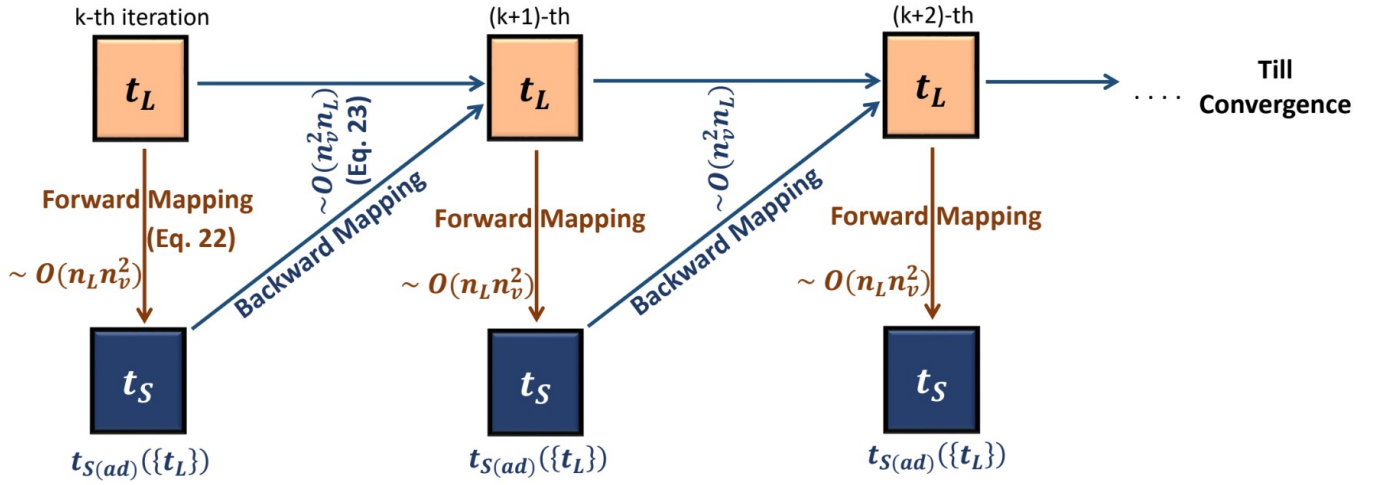


FIG. 2. A schematic representation of the circular algorithm where the auxiliary amplitudes, t_S are determined through sole function of the principal amplitudes, t_L , which are in turn updated through the back coupling of both sets of amplitudes. At each of these steps, the computational scaling goes as $n_L n_v^2 \ll n_o^2 n_v^4$.

the principal amplitude update equations as:

$$\begin{aligned} \Delta t_{L_I} = & \frac{1}{D_{L_I}} \left[(H_{L_I} + (\overline{HT})_{L_I} + (\overline{HT}_{S_i(ad)})_{L_I}) + \right. \\ & \frac{1}{2} \left((\overline{HT}_{L_J} T_{L_K})_{L_I} + (\overline{HT}_{L_J} T_{S_i(ad)})_{L_I} + \right. \\ & \left. \left. (\overline{HT}_{S_i(ad)} T_{S_j(ad)})_{L_I} \right) \right] \end{aligned} \quad (24)$$

which can be written as:

$$\Delta t_{L_I} = \frac{1}{D_{L_I}} \left(H_{L_I} + (\overline{HT})_{L_I} + \frac{1}{2} (\overline{HTT})_{L_I} \right) \quad (25)$$

where

$$T = \sum_I T_{L_I} \oplus \sum_i T_{S_i(ad)}(\{T_L\}) \quad (26)$$

This implies that both the principal and auxiliary amplitudes couple to the equations of the former. Since the contribution of the auxiliary amplitudes is significantly smaller, one may truncate the right hand side of Eq. (24) by keeping only those terms containing T_S which are overall linear. Depending on which terms are retained, we have developed two schemes. In scheme-I, all the terms in the right hand side of Eq. (24) are retained. This implies that scheme-I takes care of complete feedback coupling. In scheme-II, only terms I-IV in the right hand side of Eq. (24) are retained. In other words, the feedback of the auxiliary amplitudes in the equation of the principal amplitudes is taken up to overall linear order.

Analysis of computational scaling:

We now briefly discuss about the computational scaling associated with the determination of the auxiliary

amplitudes (Eq. (23)) and principal amplitudes (Eq. (24)). For detailed analysis of the computational scaling, we refer to one of our earlier publications²⁰. Here, for our analysis of the scaling, we would only consider the most expensive linear diagram that appears in CC theory, namely the one with all particle contraction. Such a representative diagram is shown in Fig. 1. Fig. 1(a) represents its interpretation in the context of the forward mapping via Eq. (23) where t_L amplitudes uniquely determine the t_S amplitudes. Diagrammatically, *only* the T_L operators (filled squared box, of dimension n_L) contracts with the hamiltonian (filled circles) to generate T_S . Here the index quartet of T_L , $(ijcd)$, necessarily belongs to one of the n_L elements of LAS . On the other hand, the uncontracted particle indices a, b can be arbitrary with the constraint that the uncontracted index quartet $(ijab)$ should necessarily belong to one of the SAS elements. This automatically renders the leading computational scaling for the forward mapping to be $n_L n_v^2$.

We now turn our attention to the scaling of the backward mapping (Eq. (24)). For this purpose, we resort to the diagram of the same topology as we discussed for the forward mapping, and interpret it in a different way as shown in Fig. 1(b). In this case, *all* the amplitudes are allowed to couple with the hamiltonian, however, the resulting structure should have the corresponding amplitude in LAS . This implies that the index quartet $(ijcd)$ can be any one of the principal or auxiliary amplitudes. However, the uncontracted index quartet $(ijab)$ should necessarily belong to one of the n_L elements of T_L . The restriction on the uncontracted index to the ones belonging to LAS automatically ensures that i and j cannot take any arbitrary hole orbital level. The scaling for the construction of this diagram is again $n_L n_v^2$ at the worst.

Thus the overall scaling of the scheme never exceeds $n_L n_v^2$ for the ADCC scheme, whereas, for CCD, the same

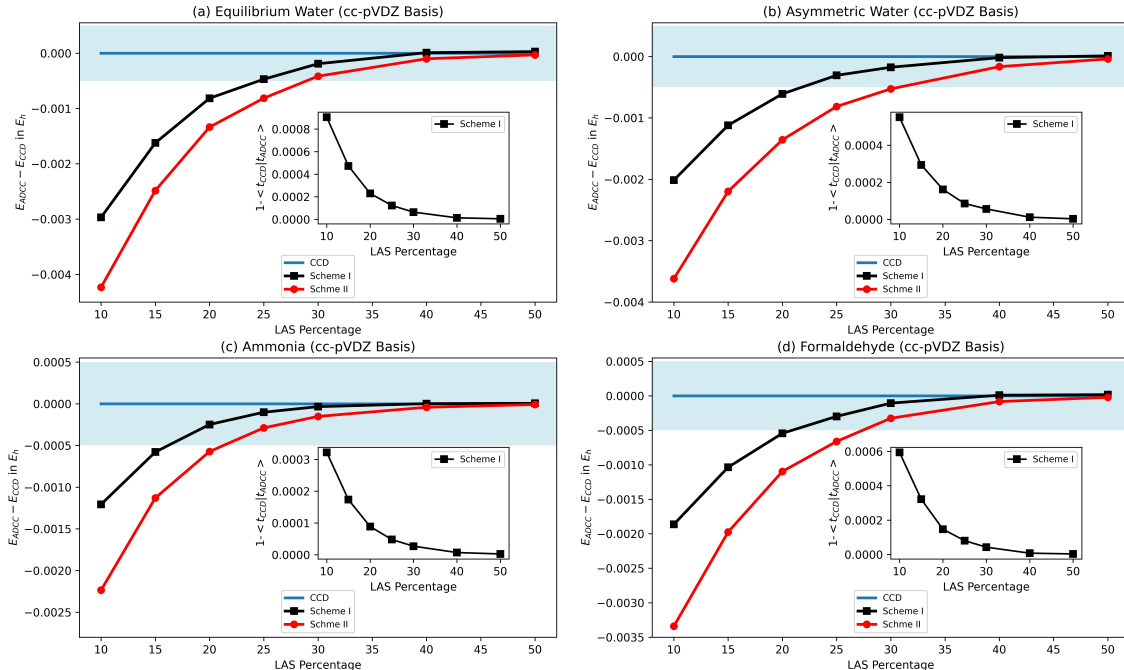


FIG. 3. Comparative study of the accuracy of ADCCD scheme-I (black line) and scheme-II (red line) against canonical CCD as functions of LAS size for four different molecules. Note that the horizontal blue line denotes the canonical CCD energy scaled to zero and the blue shaded region denotes $\pm 0.5 mE_h$ region. ADCCD scheme-I is slightly more accurate over scheme-II, particularly with smaller LAS , as expected. ADCCD scheme-I achieves $\sim 0.01 mE_h$ accuracy with only about 30 % of the total nonzero amplitudes taken as independent (principal) ones. The inset shows the accuracy of the combined set of cluster amplitudes as compared to canonical CCD and the former is shown to be as accurate as the latter with LAS taken to be 40% where one obtains accuracy up to μE_h precision.

scales as $n_o^2 n_v^4$. Since n_L is only a small fraction (vide infra) compared to $n_o^2 n_v^2$, there is a clear computational advantage of our scheme offers over the conventional one.

In summary, the overall algorithm moves in a circular manner where at each step, the auxiliary amplitudes are determined via Eq. (23) as functions of $\{t_L\}$ alone. On the other hand, the principal amplitudes, t_L are updated through complete or partial feedback coupling (for scheme-I and scheme-II, respectively) via Eq. (24). A schematic representation of the algorithm is shown in Fig. 2. Note that at each step, the scaling goes as $n_L n_v^2$. With $n_L \ll n_o^2 n_v^2$, our scheme offers significant computational savings over the conventional CC algorithm.

III. RESULTS AND DISCUSSION :

In this section, we will discuss the efficiency and accuracy of the ADCC formalism and will compare it against the canonical coupled cluster method. As a proof-of-concept, without any loss of generality, we will restrict the cluster amplitudes to only doubles (CCD). All the results are obtained with our in-house codes and the con-

vergence threshold was set to be 10^{-6} . Furthermore, no DIIS optimization is used to accelerate the convergence, even though inclusion of it is fairly straightforward.

As our objective is to simulate the canonical CCD optimization in a reduced subspace with order of magnitude less computational scaling, it is imperative to take the same as our reference. In Fig. 3, we have plotted the difference in energy obtained with ADCCD (both scheme-I and scheme-II) and canonical CCD as a function of the size of LAS . Note that the *percentage of LAS* (N) in the horizontal axis signifies that the largest $N\%$ of total nonzero amplitudes (at the MP2 level) are taken as independent parameters. Thus, a larger LAS signifies more number of principal amplitudes taken as the independent variable, against which all the remaining amplitudes (the auxiliary ones) are mapped. Note that the horizontal blue line ($y=0$) denotes the exact CCD results and the light-blue shaded region indicates a 0.5 milli-Hartree (mE_h) energy band vertically each sides of the reference energy line that provides a measure of the accuracy. Four different molecules were chosen for our application which have distinct variety of electronic complexity: (a) symmetric water (equilibrium geometry), (b) asymmet-

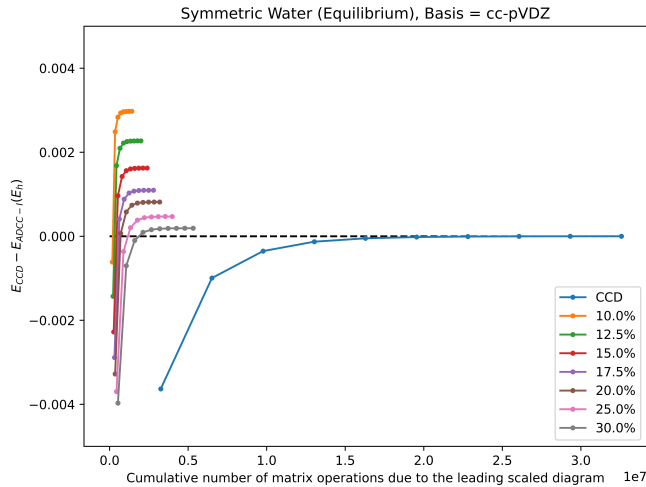


FIG. 4. Accuracy of ADCCD scheme-I for various size of LAS as function of the cumulative cost of the ADCCD calculation obtained from the highest scaling term. The blue line shows the cumulative number of matrix operation for the construction of the diagram containing all particle contraction for canonical CCD.

ric water, (c) ammonia at equilibrium geometry and (d) formaldehyde²⁹. As we expand LAS , the energy calculated from ADCCD (both scheme-I and scheme-II) converge monotonically to the corresponding CCD values. Understandably, ADCCD scheme-I is somewhat better than ADCCD scheme-II due to the fact that the former takes into account the complete feedback coupling of the auxiliary amplitudes towards the principal amplitudes, while the later does so in an approximate manner. For most of the cases, ADCCD Scheme-I enters the shaded region in between 20%-25% of LAS and acquires a remarkable accuracy of $\sim 0.1mE_h$ at around 30% in almost all the cases under consideration, while ADCCD scheme-II does so around 25%-30% and 40% of the LAS percentage, respectively. This implies that with 70% reduction in the number of independent amplitudes, ADCCD scheme-I can achieve an accuracy within tens of μE_h as compared to the canonical CCD, while ADCCD scheme-II does so with 60% reduction in the number of amplitudes. We will soon analyse how these tremendous reduction in the number of independent parameters transcends into reduction in the number of matrix operations needed to achieve the accuracy.

In the inset of each subfigure of Fig. 3, we have plotted the overlap between the adiabatically determined cluster amplitudes and the canonical cluster amplitudes. Towards this, we have mapped the amplitudes as normalized column vectors $|t_{CCD}\rangle$ and $|t_{ADCCD}\rangle$. Note that for ADCC schemes, both the principal and auxiliary amplitudes are included in $|t_{ADCCD}\rangle$ where their indexing were kept consistent. The accuracy of the ADCCD cluster amplitudes are measured by the quantity $(1 - \langle t_{ADCCD} | t_{CCD} \rangle)$. The inset plot shows the monotonic approach of the overlap value to one for scheme-I

with increase in the size of LAS , signifying that the ADCCD cluster amplitudes are of the similar accuracy to those obtained by the canonical CCD scheme.

Having discussed the precision of the optimization algorithm, we now comment on the number of matrix operations needed. While canonical CCD requires $\mathcal{O}(n_o^2 n_v^4)$ matrix operations each iterative cycle, our scheme requires $\mathcal{O}(n_L n_v^2)$ matrix operations. In Fig.4, we have demonstrated that one can achieve precision of the order of tens of μE_h with LAS taken to be 30% while it takes at least an order fewer number of cumulative matrix operations. One may note that the ADCC scheme, at each iterative cycle, requires one order of magnitude less memory compared to canonical CCD, and thus enabling large scale computations without significantly sacrificing the accuracy.

IV. CONCLUSION AND FUTURE OUTLOOK :

In this article we have rigorously established the fact that the discrete-time CC iteration dynamics can be considered as a collective motion of coexisting slow and fast relaxing modes, manifesting a dynamical hierarchical structure. Although the concepts of adiabatic elimination and slaving principle in synergetics and nonlinear dynamics are applicable for non-equilibrium systems in most of the existing literatures, borrowing these ideas we have successfully developed an equilibrium dynamical formalism (in the amplitude space) to study the complex transient behaviour of coupled cluster iteration before convergence. Our scheme shows order of magnitude reduction in computational efforts to obtain molecular ground state energy with sub- mE_h to tens of μE_h precision to the conventional CC schemes. The results are, furthermore, systematically improvable with inclusion of more number of amplitudes in the LAS . However while doing so we have neglected some higher order post-adiabatic terms that opens up scopes for further improvement of the adiabatic results²¹. Also, so far we have hived off LAS from the full cluster amplitude space purely based on the observation that the cluster amplitudes have a difference in relaxation timescales with respect to their magnitude distribution. There exist some information theoretical techniques³⁰⁻³⁵ and entropy maximization approaches^{36,37} to accurately determine the principal amplitudes. Although most of these principles are mathematically heavy and applicable for thermodynamical systems far from equilibrium, we are looking for devising our own methods based on these concepts to construct LAS in a more mathematically accurate manner. Some stochastic adiabatic elimination principles³⁸⁻⁴⁴ can also be applied to introduce stochasticity or external noise in CC to study thermal properties. We can utilise some studies that have shown how the stable and unstable manifolds can suddenly change or collide among themselves in the phase portrait under certain conditions to show some interesting phenomena^{45,46}.

In the immediate future, we will try to incorporate the higher order post-adiabatic correction terms to investigate further the intricate mathematical structures of the theory and to improve the results on top of ADCC.

V. ACKNOWLEDGMENTS

RM acknowledges the financial support from Industrial Research and Consultancy Centre, IIT Bombay, and Science and Engineering Research Board, Government of India.

DATA AVAILABILITY

The data is available upon reasonable request to the corresponding author.

KEYWORDS:

Electronic structure. Ab initio calculations. Quantum Chemistry. Nonlinear Dynamics. Synergetics.

- ¹J. Čížek, “On the correlation problem in atomic and molecular systems. calculation of wavefunction components in urchell-type expansion using quantum-field theoretical methods,” *J. Chem. Phys.* **45**, 4256–4266 (1966).
- ²J. Čížek, “On the use of the cluster expansion and the technique of diagrams in calculations of correlation effects in atoms and molecules,” *Adv. Chem. Phys.* **14**, 35–89 (1969).
- ³J. Čížek and J. Paldus, “Correlation problems in atomic and molecular systems iii. rederivation of the coupled-pair many-electron theory using the traditional quantum chemical methods,” *Int. J. Quantum Chem.* **5**, 359–379 (1971).
- ⁴R. J. Bartlett and M. Musial, “Coupled-cluster theory in quantum chemistry,” *Reviews of Modern Physics* **79**, 291 (2007).
- ⁵T. D. Crawford and H. F. Schaefer, “An introduction to coupled cluster theory for computational chemists,” *Reviews in computational chemistry* **14**, 33–136 (2000).
- ⁶P. Szakács and P. R. Surján, “Stability conditions for the coupled cluster equations,” *Int. J. Quantum Chem.* **108**, 2043–2052 (2008).
- ⁷P. Szakács and P. R. Surján, “Iterative solution of bloch-type equations: stability conditions and chaotic behavior,” *Journal of mathematical chemistry* **43**, 314–327 (2008).
- ⁸P. R. Surján, K. Simon, and Á. Szabados, “Stability analysis of the lippmann–schwinger equation,” *Molecular Physics*, e2091053 (2022).
- ⁹V. Agarwal, A. Chakraborty, and R. Maitra, “Stability analysis of a double similarity transformed coupled cluster theory,” *The Journal of Chemical Physics* **153**, 084113 (2020).
- ¹⁰M. J. Feigenbaum, “Quantitative universality for a class of nonlinear transformations,” *Journal of statistical physics* **19**, 25–52 (1978).
- ¹¹M. J. Feigenbaum, “The universal metric properties of nonlinear transformations,” *Journal of Statistical Physics* **21**, 669–706 (1979).
- ¹²V. Agarwal, S. Roy, A. Chakraborty, and R. Maitra, “Accelerating coupled cluster calculations with nonlinear dynamics and supervised machine learning,” *The Journal of Chemical Physics* **154**, 044110 (2021).
- ¹³V. Agarwal, S. Roy, K. K. Shrawankar, M. Ghogale, S. Bharathi, A. Yadav, and R. Maitra, “A hybrid coupled cluster–machine learning algorithm: Development of various regression models and benchmark applications,” *The Journal of Chemical Physics* **156**, 014109 (2022).
- ¹⁴H. Haken, “Synergetics: an overview,” *Rep. Prog. Phys.* **52**, 515–553 (1989).
- ¹⁵H. Haken and A. Wunderlin, “Slaving principle for stochastic differential equations with additive and multiplicative noise and for discrete noisy maps,” *Z. Phys. B* **47**, 179–187 (1982).
- ¹⁶A. Wunderlin, “On the slaving principle,” in *Lasers and Synergetics* (Springer, 1987) pp. 140–147.
- ¹⁷H. Haken, “Nonlinear equations. the slaving principle,” in *Advanced Synergetics: Instability Hierarchies of Self-Organizing Systems and Devices* (Springer Berlin Heidelberg, Berlin, Heidelberg, 1983) pp. 187–221.
- ¹⁸M. Born, “Born-oppenheimer approximation,” *Ann. Phys* **84**, 457–484 (1927).
- ¹⁹H. H. Synergetics, “Introduction and advanced topics,” Springer, Berlin, Heidelberg, New York Tokio **202**, 204 (1976).
- ²⁰V. Agarwal, C. Patra, and R. Maitra, “An approximate coupled cluster theory via nonlinear dynamics and synergetics: The adiabatic decoupling conditions,” *The Journal of Chemical Physics* **155**, 124115 (2021).
- ²¹H. Haken, “Higher order corrections to generalized ginzburg-landau equations of non-equilibrium systems,” *Zeitschrift für Physik B Condensed Matter* **22**, 69–72 (1975).
- ²²A. Wunderlin and H. Haken, “Generalized ginzburg-landau equations, slaving principle and center manifold theorem,” *Zeitschrift für Physik B Condensed Matter* **44**, 135–141 (1981).
- ²³S. H. Strogatz, *Nonlinear dynamics and chaos: with applications to physics, biology, chemistry, and engineering* (CRC press, 2018).
- ²⁴K. T. Alligood, T. D. Sauer, and J. A. Yorke, “Two-dimensional maps,” *Chaos: An Introduction to Dynamical Systems*, 43–104 (1996).
- ²⁵L. Lam, *Introduction to nonlinear physics* (Springer Science & Business Media, 2003).
- ²⁶G. Schmidt, “Haken, h., advanced synergetics. instabilities of self-organizing systems and devices. berlin-heidelberg-new york-tokyo, springer-verlag 1983. xv. 356 s., 105 abb., dm 98,ãĀĀ. us \$38.90. isbn 3-540-12 162-5 (springer series in synergetics 20),” *Zeitschrift Angewandte Mathematik und Mechanik* **65**, 394–394 (1985).
- ²⁷H. Haken, “Nonlinear equations. the slaving principle,” in *Advanced Synergetics* (Springer, 1983) pp. 187–221.
- ²⁸H. Haken, “Discrete dynamics of complex systems,” *Discrete Dynamics in Nature and Society* **1**, 1–8 (1997).
- ²⁹R. D. Johnson *et al.*, “Nist computational chemistry comparison and benchmark database,” <http://srdata.nist.gov/cccbdb> (2006).
- ³⁰H. Haken and J. Portugali, “Information and self-organization,” (2016).
- ³¹H. Haken, “Application of the maximum information entropy principle to selforganizing systems,” *Zeitschrift für Physik B Condensed Matter* **61**, 335–338 (1985).
- ³²H. Haken, “Self-organization and information,” *Physica Scripta* **35**, 247 (1987).
- ³³H. Haken, *Information and self-organization: A macroscopic approach to complex systems* (Springer Science & Business Media, 2006).
- ³⁴H. Haken and J. Portugali, “Information and self-organization ii: Steady state and phase transition,” *Entropy* **23**, 707 (2021).
- ³⁵H. Haken, “Information, information gain, and efficiency of self-organizing systems close to instability points,” *Zeitschrift für Physik B Condensed Matter* **61**, 329–334 (1985).
- ³⁶H. Haken, “The maximum entropy principle for non-equilibrium phase transitions: Determination of order parameters, slaved modes, and emerging patterns,” *Zeitschrift für Physik B Condensed Matter* **63**, 487–491 (1986).
- ³⁷H. Haken, “Synergetics: an overview,” *Reports on Progress in Physics* **52**, 515 (1989).

- ³⁸G. Schöner and H. Haken, “The slaving principle for stratonovich stochastic differential equations,” *Zeitschrift für Physik B Condensed Matter* **63**, 493–504 (1986).
- ³⁹G. Schöner and H. Haken, “A systematic elimination procedure for ito stochastic differential equations and the adiabatic approximation,” *Zeitschrift für Physik B Condensed Matter* **68**, 89–103 (1987).
- ⁴⁰H. Aoki and K. Kaneko, “Slow stochastic switching by collective chaos of fast elements,” *Physical review letters* **111**, 144102 (2013).
- ⁴¹D.-j. Wu and L. Cao, “Relations between different representations of stochastic adiabatic solutions,” *Zeitschrift für Physik B Condensed Matter* **81**, 451–455 (1990).
- ⁴²G. W. Constable, A. J. McKane, and T. Rogers, “Stochastic dynamics on slow manifolds,” *Journal of Physics A: Mathematical and Theoretical* **46**, 295002 (2013).
- ⁴³J.-H. Li, L. Cao, and D.-J. Wu, “Relations of systematic adiabatic approximation and stochastic adiabatic approximation,” *Communications in Theoretical Physics* **18**, 403 (1992).
- ⁴⁴S. Wu, K. He, and Z. Huang, “Suppressing complexity via the slaving principle,” *Physical Review E* **62**, 4417 (2000).
- ⁴⁵C. Grebogi, E. Ott, and J. A. Yorke, “Crises, sudden changes in chaotic attractors, and transient chaos,” *Physica D: Nonlinear Phenomena* **7**, 181–200 (1983).
- ⁴⁶K. Takatsuka, “Adiabatic and nonadiabatic dynamics in classical mechanics for coupled fast and slow modes: sudden transition caused by the fast mode against the slaving principle,” *Molecular Physics* **116**, 2556–2570 (2018).